Michigan State University

National Superconducting Cyclotron Laboratory

ENTRANCE CHANNEL EFFECTS AND THE FORMATION OF HOT NUCLEI

H.M. XU, W.G. LYNCH, P. DANIELEWICZ, and G.F. BERTSCH

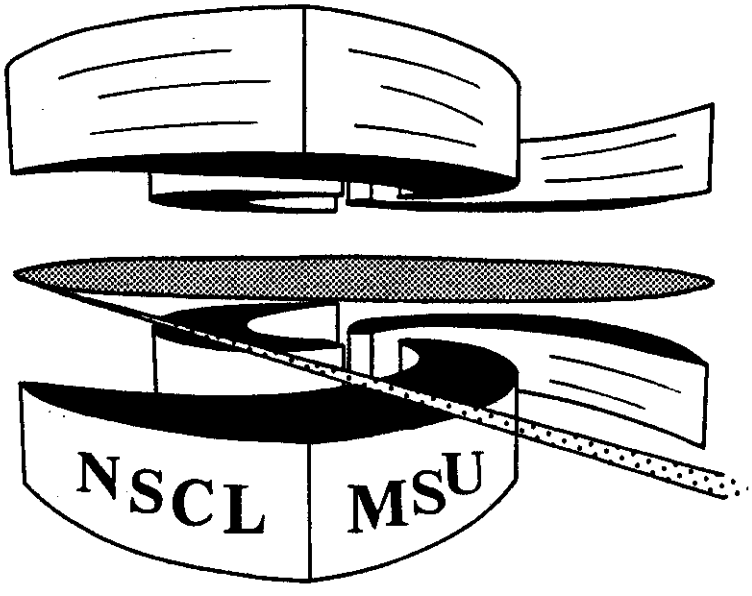

MSUCL-765 **MARCH 1991**

MSUCL-765
March, 1991

Entrance Channel Effects and the Formation of Hat Nuclei

H.M. Xu, W.G. Lynch, P. Danielewicz and G.F. Bertsch

National Superconducting Cyclotron Laboratory and Department of Physics, Michigan State University, East Lansing, Michigan 48824.

With an improved Boltzmann-Uehling-Uhlenbeck code, we have calculated the excitation energies and the angular momenta of heavy composite residues Formed in $^{40}Ar+^{27}Al$ collisions. At E/A≥35 MeV, the maximum residue angular momenta are predicted to be significantly smaller than the static limits predicted by the liquid drop model. The excitation energy of residues produced in central collisions is predicted to increase with incident energy, reaching a Value of about 5-6 MeV/nucleon at E/A=40 MeV.

The formation and the subsequent decay of hot nuclear systems have been extensively studied in nucleus-nucleus collisions at energies between E/A =15 and 100 MeV.[1-21] One challenging goal of such studies is to determine the thermal and dynamical limits of hot composite systems formed in the collisions.[1-27] Calculations predict that metastable composite nuclei cannot exist at temperatures in excess of five to ten MeV.[23-27] The maximum or "limiting" temperature of metastable nuclei is predicted to be sensitive to the nuclear equation of state (EOS) and the temperature dependence of the liquid drop surface energy.[23]

Experimental investigations of the stability of hot nuclei have reported two striking observations. The cross sections for fusion-like processes appear to vanish at incident energies E/A≥35 MeV.[1-5,7,10-13] Measurements of residue velocities, multiplicities of evaporated particles and populations of excited states of emitted fragments suggest that there are limits to the excitation energies of hot nuclear systems.[1-15] Simple model calculations, which relate the vanishing cross sections, residue velocities, particle spectra and multiplicities, to the predictions of liquid drop calculations, support the interpretation of this experimental data in terms of a "limiting temperature" for hot nuclei.[1-4,6-13]

Interpretations of residue observables in terms of a "limiting temperature" focus upon the stability of hot nuclei and do not address questions concerning their formation. To investigate dynamical limits to the excitation energies and angular momenta of hot residual nuclei, we performed calculations for $^{40}Ar+^{27}Al$ collisions using the Boltzmann-Uehling-Uhlenbeck (BUU) equation. We find that the maximum calculated residue angular momenta decrease much faster with incident energy than expected from rotating liquid drop model calculations. The calculated residue excitation energies are sensitive to the nuclear equation of state

(EOS) and effective nucleon-nucleon cross section. Similar to results obtained for simulations of other light systems,[17-22] the residue excitation energies increase slightly with incident energy, reaching values of about $E^*/A \approx 5$-6 MeV at E/A = 40 MeV. At all incident energies, the residue excitation energies are considerably less than the values expected for complete fusion.

The calculations were performed by solving the BUU equation[28,29] in the lattice Hamiltonian approximation.[30] The mean field potential in these calculations included Coulomb and symmetry energy terms and an isoscalar mean field for which the compressibility was varied.[31] For simplicity, the in-medium nucleon-nucleon cross section in the BUU equation was taken to be isotropic and energy independent.[29] The mean field and the Pauli blocking factors in the collision integral were calculated with distribution functions ensemble averaged over 80 parallel simulations. Over an elapsed time of 300 fm/c, the calculated total energy and total angular momentum are conserved to within 0.1 MeV/nucleon and 6%, respectively. Two parameter sets 1) a soft EOS (nuclear compressibility K = 200 MeV) and an in medium nucleon-nucleon cross section, $\sigma_{NN}=\int d\Omega \sigma_{NN}(\Omega)$ = 50 mb; and 2) a stiff EOS (K =380 MeV) and σ_{NN} = 25 mb were used in these calculations. These parameter sets have not been adjusted to reproduce experimental observables. Both parameter sets predict essentially equal residue cross sections for $^{40}Ar+^{27}Al$ collisions at incident energies E/A =25-40 MeV,[31] with an energy dependence of the residue cross sections qualitatively similar to that observed experimentally.

1. The Freezeout Criterion

Since the residue continues to decay after its formation, the residue masses, excitation energies and angular momenta are sensitive to the freezeout time at which observables are evaluated. To indicate how this freezeout time was chosen, we show, in Fig. 1, the decomposition of excitation energy following Remaud et al[19,21] for $^{40}Ar+^{27}Al$ collisions at E/A=30 MeV with the soft EOS. At t≈40 fm/c, one observes a maximum in the thermal excitation energy. This maximum is an artifact of the initial momentum distributions, in which the longitudinal velocities of the projectile and the target nuclei cancel each other, causing a minimum in the computation of the collective energy. After t≈40 fm/c, the system expands for a while and then contracts back, exhibiting a monopole-like vibration.[19] At t≈120 fm/c, one can see a local maximum in the thermal excitation energy. At this time, the preequilibrium emission has just completed,[19] and after this time, the thermal energy gradually decreases. Indeed, if one plots the number of particles emitted as a function of time, one observes a change in emission rate at t≈120 fm/c, with a high rate for fast emission at the earlier stage and a low rate characteristic for slow evaporation at the later stage. We therefore choose t≈120 fm/c as the thermal freeze-out time for the heavy residues at this energy (for the stiff EOS, this criterion gives 100 fm/c).

2. Collisions at E/A=30 MeV

In Fig. 2, different components of excitation energy at the freezeout are plotted as functions of impact parameter for $^{40}Ar+^{27}Al$ at E/A=30 MeV, for the two parameter sets discussed in the introduction. The solid symbols represent calculations where a single heavy residue is observed in the final state. The open symbols represent calculations at larger impact

parameters where the system breaks up eventually into projectile-like and the target-like residues. The total excitation energy (solid circles) increases slightly with impact parameter, an effect which is partly due to the collective energy of rotation. To understand this increase, we decomposed the total excitation energy into contributions from thermal and collective motion.[19] Using a rigid-body moment of inertia obtained numerically from the residue density distribution, we estimated a collective energy of rotation. Subtracting this from the total excitation energy leaves one with the values depicted by the crosses in Fig. 2. Some of the remaining excitation energy is actually an increase in the potential energy because the residue is at subnuclear density. The diamonds show the excitation energy which remained after the rotational energy and the potential energy of expansion have been subtracted.

The energy due to collective motion in the residue can be more accurately estimated by defining a collective velocity field on the computational lattice,[19] and integrating the kinetic energy of collective motion over the lattice. This provides a total collective energy which is about 0.5 - 1.0 MeV/A larger than the rotational energy for impact parameters which produce heavy residues. At larger impact parameters where residues are not formed, the total collective energy increases strongly with impact parameter reflecting an incomplete dissipation of the incident collective motion of projectile and target nucleons into other degrees of freedom.

The thermal excitation energy is obtained by subtracting both the total collective energy and the potential energy associated with expansion. The thermal energy, designated by the squares, is smaller for larger impact parameters, where residue formation is less likely. This suggest that the

formation of heavy residues in these calculations is not simply related to the stability of the residual nucleus under the increase of temperature.

3. Residue Angular Momenta

At each incident energy, the maximum residue angular momentum occurs at the largest impact parameter, $b=b_{max}$, for which a single residue can be formed. In Fig. 3, we display the energy dependence of the residue angular momenta (bottom windows) and masses (top windows) near $b=b_{max}$ for the soft equation of state (right-hand side) and the stiff equation of state (left-hand side). For each incident energy, the solid symbol provides the residue angular momentum for the largest impact parameter at which a fused residue is observed. The open symbols provide the angular momenta at slightly larger impact parameters where the system eventually breaks up into two fragments. For $E/A \lesssim 35$ MeV and both parameter sets, the maximum calculated residue angular momenta are comparable to those predicted by the rotating liquid-drop model,[32] shown here by the solid curves. Above $E/A \approx 35$ MeV, however, the maximum angular momenta fall below the rotating liquid-drop model predictions. At these energies, residues with angular momenta near the liquid drop limits are not formed, due in part to an incomplete damping of incident collective motion for $b>b_{max}$.

4. The Variation of the Excitation Energy With Incident Energy

On the left hand side of Fig.4, we show the decomposition of the excitation energy for central collisions as a function of incident energy for the soft EOS (top panel) and the stiff EOS (bottom panel). On the right hand side, we provide the corresponding calculations for the maximum impact parameters b_{max} that lead to residue formation. With both equations of state and both impact parameters, the calculated total excitation energy

and the thermal excitation energy increase only slightly with incident energy, a phenomenon also predicted in other simulations of light systems.[17,22] The calculated excitation energies are generally larger for calculations with the stiff EOS, a trend also predicted by static models,[23] even though σ_{NN} was adjusted to make equal residue cross sections for the two sets of parameters.[31] The total excitation energy for the stiff EOS increases gradually from $E^*/A \approx 3.8$ MeV at E/A=25 MeV to $E^*/A \approx 5.5$ MeV at E/A=40 MeV; the thermal energy increases correspondingly from $E^*/A \approx 2.4$ to 2.8 MeV. The maximum thermal excitation energy, $E^* \approx 2.8$ MeV, is comparable to predictions for the maximum excitation energy that a non-rotating nucleus can sustain;[25-27] thus additional reductions in the calculated residue cross sections may occur for central collisions at the highest energies due to thermal instabilities[23-27] of the hot residues which are not considered by our calculations.

Detailed comparisons of these calculations to experimental data are premature because the nucleon-nucleon cross section was not chosen to optimize the agreement with the experimental observables. The calculated observables are also influenced by the neglect of fluctuations and cluster emission within the BUU approach. Such processes will render the present abrupt transition at b_{max} from fusion-like to peripheral collisions more gradual. Residue velocity distributions are very sensitive to this transition, and are consequently not described accurately for these light systems. Comparisons with a reduced sensitivity to large impact parameter collisions may be possible with heavier asymmetric entrance channels [6,12-14]; calculations to explore these questions for such systems are needed. Because residue velocity distributions are sensitive to cluster production, we cannot address the similarity of our calculated excitation energies to those estimated from experimentally measured residue velocity

distributions using massive transfer models.[1-4,6-13] Excitation energies deduced from the calculated residue velocities using the massive transfer model are shown as the open points in Fig. 4. The present BUU calculations are inconsistent with massive transfer model, largely because the massive transfer model assumes less cooling due to preequilibrium emission than is predicted by the BUU calculations.

5. Summary

In conclusion, we have investigated, with an improved BUU model, excitation energies and angular momenta of heavy residues formed in the $^{40}Ar+^{27}Al$ collisions. We find that the maximum residue angular momenta are comparable to the liquid drop predictions at E/A≤30 MeV and fall below the liquid drop predictions at higher incident energies. At larger impact parameters where residues are not formed, the collective energies of projectile and target appear to be incompletely damped. This dynamical effect appears to limit the calculated residue cross sections at E/A≥35 MeV. The calculated excitation energy for central collisions increases with incident energy, reaching a value of 5.5 MeV/nucleon at E/A =40 MeV with the stiff EOS and σ_{NN}=25 mb, lower than the value inferred from the residue velocity using massive transfer models. The calculated thermal energies are comparable to predictions for the maximum excitation energy that a nucleus can sustain, thus thermal instabilities in central collisions could remove additional flux from the fusion cross sections, particularly, in the high energy regions where the fusion cross sections vanish rapidly.

The present calculations have several limitations. Because the theory has insufficient fluctuations,[17,21,28] it can only predict mean values of observables for which fluctuations play a small role. It can not predict, for example, how and under what conditions fluctuations will cause

the hot residues to disassemble. Further investigations are also required to assess the sensitivity of the detail algorithm of Pauli-blocking and of surface energy to experimental observables.

We would like to acknowledge many helpful and fruitful discussions with M. Tohyama, C.K. Gelbke and M.B. Tsang. One of us (HMX) acknowledges enlightening discussions with B. Remaud. Another of us (WGL) acknowledges a receipt of a NSF Presidential Young Investigator Award. This work was supported by the National Science Foundation under Grant Nos. PHY-86-11210, PHY-87-14432, and PHY-89-05933.

References

1. E. Suraud, C. Gregoire, and B. Tamain, Prog. Part. Nucl. Phys., 23 (1989) 357.
2. D. Guerreau, Proceedings of the NATO workshop on Nuclear Matter and Heavy Ion Collisions, NATO ASI Series B: Physics Vol. 205, p. 187 (1989) Plenum Press.
3. S. Leray, J. Phys. Colloq. 47, C4 (1986) 275.
4. G. Auger, et al., Phys. Lett. B 169 (1986) 161.
5. H. Nifenecker, et al., Nucl. Phys. A447 (1985) 533c.
6. R. Wada, et al., Phys. Rev. C39 (1989) 497.
7. P. Decowski, et al., Proceedings of the XXVIII International Winter Meeting on Nuclear Physics, Bormio, Italy, Jan., 22-26, 1990.
8. K.A. Griffioen et al., Phys. Lett. B 237 (1990) 24
9. W. Bohne, et al, Phys. Rev. C41 (1990) R5.
10. A. Fahli, et al, Phys. Rev. C34 (1986) 161.
11. B. Bourderie and M.F. Rivet, Z. Phys. A321 (1985) 703.
12. D. Fabris, et al, Nucl. Phys. A471 (1987) 351c.
13. D. Jaquet, et al, Phys. Rev. Lett. 53 (1984) 2226.
14. J. Galin, Nucl. Phys. A488 (1988) 297c.
15. Z. Chen, et al., Phys. Rev. C36 (1987) 2297.
16. B. Remaud, et al., Phys. Lett. B 180 (1986) 198.
17. K. Sneppen and L. Vinet, Nucl. Phys. A480 (1988) 342
18. W. Bauer, et al, Phys. Rev. Lett. 58 (1987) 863.
19. B. Remaud, et al., Nucl. Phys. A488 (1988) 423c.
20. S. Bhattacharya, Phys. Rev. Lett. 62 (1989) 2589.
21. E. Suraud, et al, Phys. Lett. B229 (1989) 359.
22. D. Boal, J. Glosli, and C. Wicentowich, Phys. Rev. C40 (1989) 601.

23. S. Levit and P. Bonche, Nucl. Phys. A437 (1984) 426.

24. H. Sagawa, and G.F. Bertsch, Phys. Lett. B155 (1985) 11.

25. D.H.E. Gross, Nucl. Phys. A471, (1987) 339.

26. J. Bondorf et al., Nucl. Phys. A444 (1985) 460.

27. W.A. Friedman, Phys. Rev. Lett. 60 (1988) 2125.

28. G.F. Bertsch, H. Kruse, and S. Das Gupta, Phys. Rev. C29 (1984) 673; G.F. Bertsch, and S. Das Gupta, Phys. Rep. 160 (1988) 189, and references contained therein.

29. J. Aichelin and G. Bertsch, Phys. Rev. C31 (1985) 1730.

30. R.J. Lenk and V.R. Pandharipande, Phys. Rev. C39 (1989) 2242.

31. H.M. Xu, et al., Phys. Rev. Lett. 65 (1990) 843.

32. S. Cohen, F. Plasil, and W. J. Swiatecki, Ann. Phys. (New York) 82 (1974) 557 .

Fig. 1: A decomposition of the total energy per nucleon into the potential energy (bottom line), Fermi energy associated with the Pauli exclusion principle (difference between the bottom and second lines), kinetic energy of emitted particles (difference between the second and third lines), collective energy of bound nucleons (difference between the third and fourth lines) and thermal energy (difference between the fourth and fifth lines). The freezeout time is indicated by the dotted line.

Fig.2 : A decomposition of the predicted excitation energy at freezeout for different impact parameters in $^{40}Ar+^{27}Al$ collisions, assuming the soft EOS (top panel) or the stiff EOS (lower panel). The solid and open symbols are explained in the text. The solid lines are drawn to guide the eye.

Fig.3 : Residual masses (top) and angular momenta (bottom) at b_{max} are plotted at freezeout as functions of the incident energy for calculations with the soft EOS (left side) or the stiff EOS (right side), Here, b_{max}= 4.7, 4.0, 3.3, 2.4 fm (5.0, 4.3, 2.0, 1.2 fm) at E/A = 25, 30, 35, 40 MeV, for calculations with the soft (stiff) EOS, respectively. The curves and the open and solid symbols are explained in the text.

Fig.4 : Decompositions of the excitation energy at freezeout for b=0 fm (left side), $b=b_{max}$ (right side), soft EOS (top panel) and stiff EOS (lower panel) as functions of the incident energy for $^{40}Ar+^{27}Al$ collisions. Here, the solid circles and squares denote the total and thermal excitation energies, respectively. The dashed line designates predictions of the massive transfer model using our calculated residue velocity.

MSU-90-211

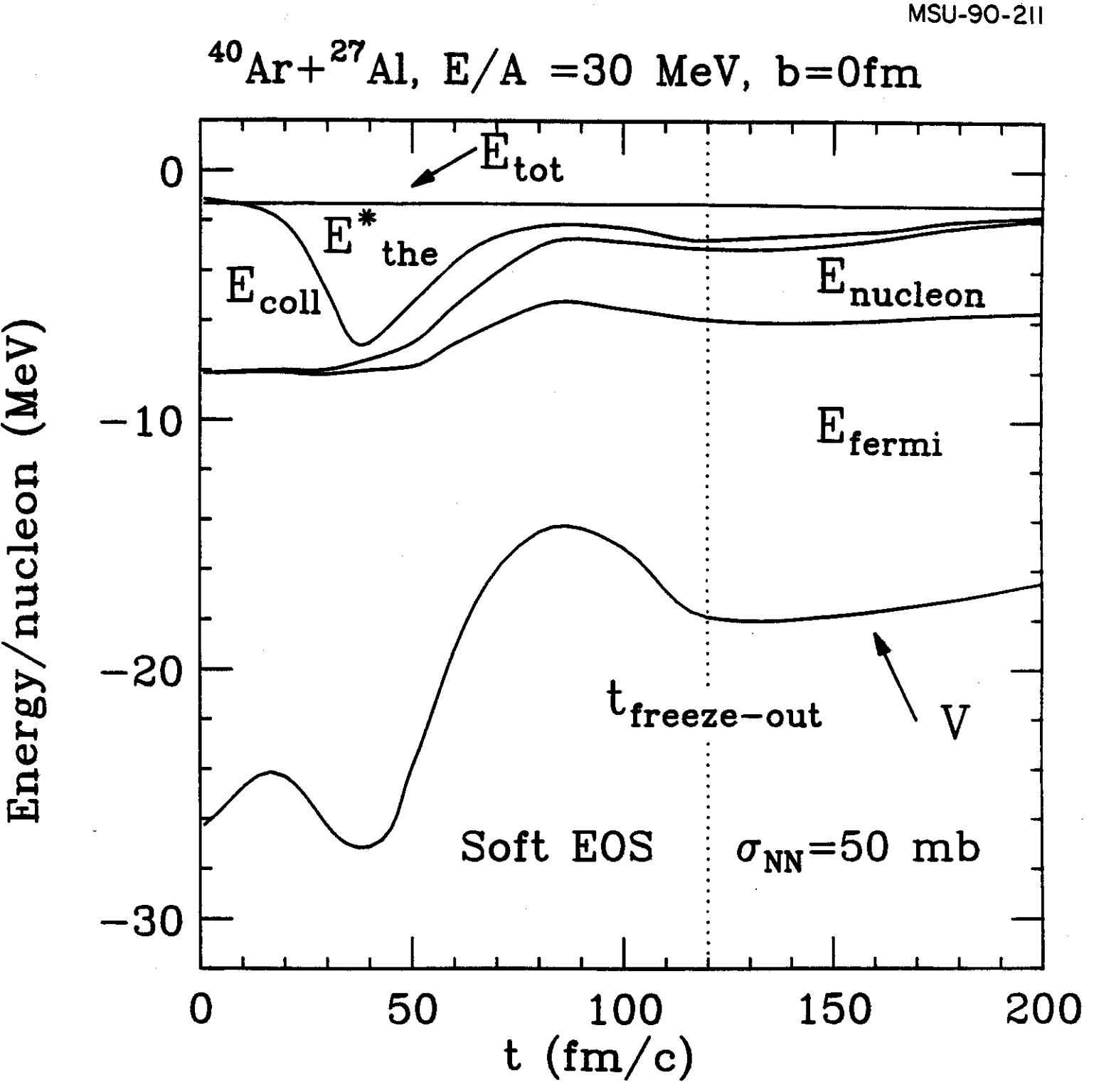

Fig. 1

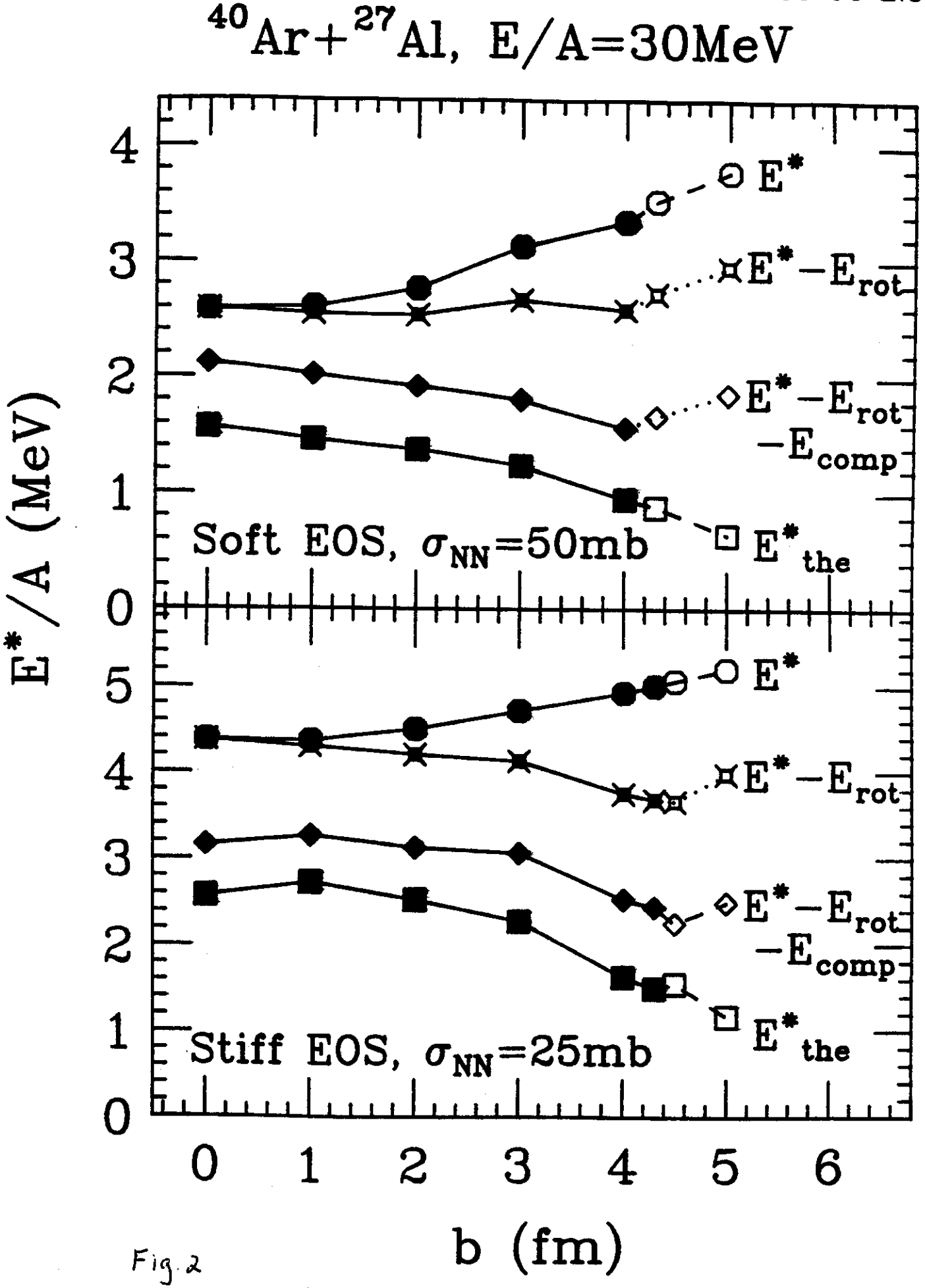
$^{40}Ar+^{27}Al$, E/A=30MeV
E^*/A (MeV)
E^*
E^*-E_{rot}
$E^*-E_{rot}-E_{comp}$
E^*_{the}
Soft EOS, σ_{NN}=50mb
Stiff EOS, σ_{NN}=25mb
b (fm)

Fig. 2

MSU-90-112

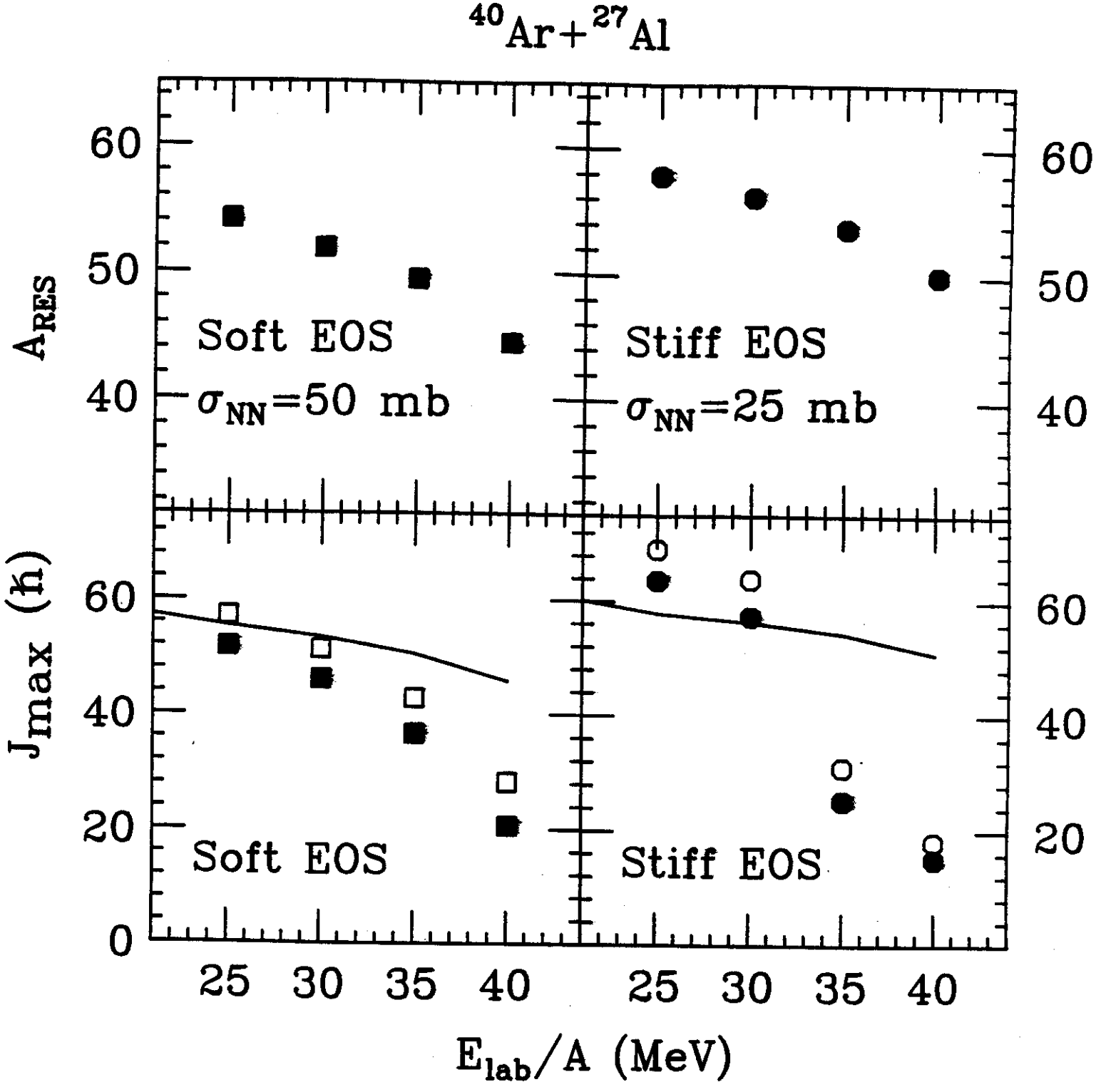

Fig. 3

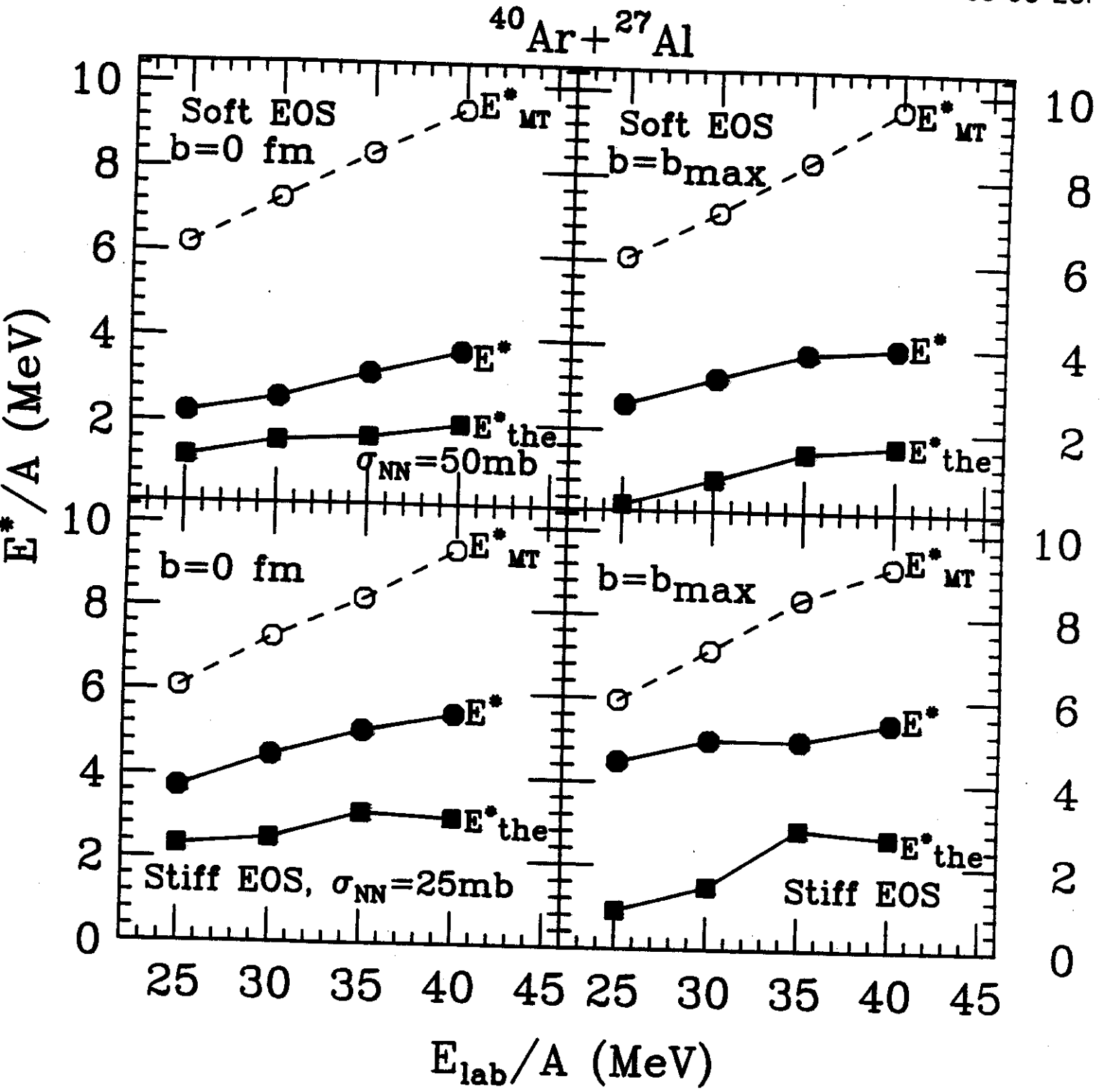
$^{40}Ar+^{27}Al$
Soft EOS
b=0 fm
Soft EOS
b=b_{max}
b=0 fm
b=b_{max}
Stiff EOS, σ_{NN}=25mb
Stiff EOS
σ_{NN}=50mb
E^*_{MT}
E^*
E^*_{the}
E^*/A (MeV)
E_{lab}/A (MeV)
0
2
4
6
8
10
25
30
35
40
45

Fig. 4